



Multi-objective design optimization using cascade evolutionary computations

Nikos D. Lagaros, Vagelis Plevris, Manolis Papadrakakis *

*Institute of Structural Analysis and Seismic Research, National Technical University of Athens, 9, Iroon Polytechniou Str.,
Zografou Campus, GR-15780 Athens, Greece*

Received 20 June 2004; received in revised form 10 November 2004; accepted 29 December 2004

Abstract

The consideration of uncertainties in conjunction with the probability of violation of the constraints imposed by the design codes is examined in the framework of structural optimization. The optimum design achieved based on a deterministic formulation is compared, in terms of the optimum weight, the probability of violation of the constraints and the probability of failure, with the optimum designs achieved through a robust design formulation where the variance of the response is considered as an additional criterion. The stochastic finite element problem is solved using the Monte Carlo Simulation method, combined with the Latin Hypercube Sampling technique for improving its computational efficiency. A non-dominant cascade evolutionary algorithm-based methodology is adopted for the solution of the multi-objective optimization problem encountered, in order to obtain the global Pareto front curve.

© 2005 Elsevier B.V. All rights reserved.

Keywords: Multi-objective optimization; Latin hypercube; Robust design optimization; Cascade evolutionary algorithms

1. Introduction

In deterministic-based structural sizing optimization problems the aim is to minimize the weight or the cost of the structure taking into account certain behavioral constraints, mainly on stresses and displacements, as imposed by the design codes. On the other hand, stochastic performance measures are increasingly being taken into consideration in many contemporary engineering applications that involve various reliability requirements. Reliability is defined as the probability that a system will meet the design demands

* Corresponding author. Tel.: +30 210 7721694; fax: +30 210 7721693.

E-mail addresses: nlagaros@central.ntua.gr (N.D. Lagaros), vplevris@central.ntua.gr (V. Plevris), mpapadra@central.ntua.gr (M. Papadrakakis).

during its life time. In structural optimization, stochastic performance measures can be taken into account using two distinct formulations, Robust Design Optimization (RDO) and Reliability-Based Design Optimization (RBDO) [9]. According to the RDO formulation the objective is to minimize the influence of the stochastic variation of some structural parameters on the design, while the main goal in the RBDO formulation is to achieve optimum design with respect to extreme uncertain events.

Although a great deal of studies has been proposed during the last three decades for structural optimization, those devoted to RDO are rather limited. Chen and Lewis [2] presented some preliminary results of robust design for multi-disciplinary optimization applying efficient methods for the uncertainty analysis. Lee and Park [12] solved a RDO problem where the multi-objective problem considered had two criteria to be minimized, the mean value and the standard deviation of the structural weight. The multi-objective problem was solved using the weighting sum method in the context of a mathematical programming algorithm. Sandgren and Cameron [21] proposed a hybrid genetic/non-linear programming algorithm for the solution of the multi-objective problem in the framework of RDO. Messac and Ismail-Yahaya [16] developed the flexible physical programming-based RDO methodology that formulates the RDO problem in terms of physically meaningful design performance degradation levels. Jung and Lee [11] incorporated the probability of feasibility into the RDO problem, where each probability constraint was transformed into a sub-optimization problem by the advanced first-order second moment method. Doltsinis and Kang [5] dealt with the RDO problem considering the minimization of the mean value and the standard deviation of a nodal displacement and treating the structural weight as a constraint function. Papadrakakis et al. [19] studied a RDO problem where both the weight of the structure and the variance of the structural response were minimized, while the Linear Weighting Sum (LWS) method was used for the solution of the multi-objective optimization problem.

In the present work, the non-dominant Cascade Evolutionary Algorithm (CEA)-based multi-objective optimization scheme is proposed for the solution of structural RDO problems, together with an improved handling of the multi-objective optimization problem, and is compared to the LWS method. The stochastic finite element problem is solved using the Monte Carlo simulation method combined with the Latin Hypercube Sampling (LHS) technique in order to reduce the number of simulations needed for the calculation of the required statistical quantities. Up to a hundred LHS simulations proved to be sufficient, for the test cases considered for calculating the statistical quantities. Furthermore, the advantages of the proposed cascade multi-objective optimization methodology over the classical LWS method and the importance of considering the variance of the structural response as a criterion are demonstrated. Two real-scale truss structures have been examined subject to constraints imposed by the Eurocode 3 [8].

The paper is organized as follows: in Section 2, the formulation and solution of the stochastic finite element problem is described. The next section presents the multi-objective optimization problem and the description of the methodology adopted which encompasses non-dominant search, cascade evolutionary computations and the Tchebycheff metric. Subsequently, in Section 4 the definition of a RDO problem is given. The numerical tests, that demonstrate the potential of the proposed multi-objective optimization scheme in solving realistic problems compared to the LWS method, are presented in Section 5 together with a verification of the efficiency of LHS. A comparative study between DBO and RDO optimum solutions is also given in Section 5, followed by the concluding remarks in Section 6.

2. Stochastic finite element analysis

During the last two decades much progress has been achieved on stochastic finite element methods [20,22]. However, comparatively few studies have been performed in structural optimization taking into account uncertain parameters.

2.1. Stochastic response basics

In this work several parameters that affect the structural performance, such as the modulus of elasticity, yield stress and applied loading have been considered as uncertain variables. Let n_r be the total number of the uncertain variables considered and \mathbf{r} is the corresponding vector. The stochastic finite element equation that has to be solved can be stated as follows

$$\mathbf{K}(\mathbf{r})\mathbf{u}(\mathbf{r}) = \mathbf{p}(\mathbf{r}), \quad (1)$$

where $\mathbf{K}(\mathbf{r})$ is the global uncertain stiffness matrix, $\mathbf{u}(\mathbf{r})$ is the vector of nodal displacements and $\mathbf{p}(\mathbf{r})$ is the loading vector. The statistical quantities that are usually required in the framework of a RDO problem are the mean value and/or the variance of the objective function, such as the weight, or the structural response. If the uncertain variables \mathbf{r} are not correlated with each other, as it is assumed in this work, the mean value \bar{u}_i and the variance $\sigma_{u_i}^2$ of the displacement of the i th degree of freedom can be calculated as follows

$$\bar{u}_i = \int \int \cdots \int u_i(\mathbf{r}) \text{pdf}_1(r_1) \cdots \text{pdf}_{n_r}(r_{n_r}) \, d\mathbf{r}, \quad (2a)$$

$$\sigma_{u_i}^2 = \int \int \cdots \int [u_i(\mathbf{r}) - \bar{u}_i]^2 \text{pdf}_1(r_1) \cdots \text{pdf}_{n_r}(r_{n_r}) \, d\mathbf{r}, \quad (2b)$$

where $\text{pdf}_j, j = 1, \dots, n_r$, is the probability density function of the j -th uncertain variable. For the solution of the problem of Eq. (1) which results in the calculation of the statistical quantities of Eqs. (2a) and (2b), a number of methods have been proposed that can be classified into statistical and non-statistical ones. In this work, a statistical method and in particular Monte Carlo Simulation combined with the Latin Hypercube Sampling is employed.

2.2. Monte Carlo Simulation (MCS) method

The MCS method is particularly applicable for the stochastic analysis of structures when an analytical solution is not attainable. This is mainly the case in problems of complex nature with a large number of uncertain variables, where all other stochastic analysis methods are inapplicable. Despite the fact that the mathematical formulation of the MCS is simple, the method has the capability of handling practically every possible case regardless of its complexity and the variation of the uncertain variables. The MCS method has proven to be efficient [18] for the calculation of the statistical quantities in the framework of a RBDO problem.

For the structural stochastic analysis problems examined in this study, the probability of violation of the behavioral constraints and the probability of failure are calculated along with the mean value and the variance of a characteristic nodal displacement that represents the response of the structure. Expressing the limit state function as $G(\mathbf{r}) < 0$, the probability of violation of the behavioral constraints can be written as

$$p_{\text{viol}} = \int_{G(\mathbf{r}) \geq 0} f_r(\mathbf{r}) \, d\mathbf{r}, \quad (3)$$

where $f_r(\mathbf{r})$ denotes the joint probability of violation. A similar expression is used for the probability of failure.

Since MCS is based on the theory of large numbers (N_∞), an unbiased estimator of the probability of violation, the mean value and the variance of the nodal displacement in question is given by

$$p_{\text{viol}} = \frac{1}{N_\infty} \sum_{j=1}^{N_\infty} I(\mathbf{r}_j), \quad (4a)$$

$$\bar{u}_i = \frac{1}{N_\infty} \sum_{j=1}^{N_\infty} u_i(\mathbf{r}_j), \tag{4b}$$

$$\sigma_{u_i}^2 = \frac{1}{N_\infty} \sum_{j=1}^{N_\infty} [u_i(\mathbf{r}_j) - \bar{u}_i]^2, \tag{4c}$$

where \mathbf{r}_j is the j th vector of the random structural parameters, and $I(\mathbf{r}_j)$ is an indicator for successful and unsuccessful simulations defined as

$$I(\mathbf{r}_j) = \begin{cases} 1 & \text{if } G(\mathbf{r}_j) \geq 0, \\ 0 & \text{if } G(\mathbf{r}_j) < 0. \end{cases} \tag{5}$$

In order to estimate \bar{u}_i and $\sigma_{u_i}^2$ from Eqs. (4b) and (4c) an adequate number of N independent random samples is produced, while p_{viol} is given in terms of sample mean by

$$p_{\text{viol}} \cong \frac{N_H}{N}, \tag{6}$$

where N_H is the number of successful simulations and N is the total number of simulations. The probability of failure is calculated using a similar estimator of Eqs. (4a) and (6).

2.3. Latin Hypercube Sampling

The Latin Hypercube Sampling (LHS) method was introduced by MacKay et al. [15] in an effort to reduce the required computational cost of purely random sampling methodologies. Latin hypercube sampling is a strategy for generating random sample points ensuring that all portions of the random space in question are properly represented. LHS is generally recognized as one of the most efficient size reduction techniques. The basis of LHS is a full stratification of the sampled distribution with a random selection inside each stratum. In consequence, sample values are randomly shuffled among different variables. A Latin hypercube sample is constructed by dividing the range of each of the n_r uncertain variables into N non-overlapping segments of equal marginal probability. Thus, the whole parameter space, consisting of N parameters, is partitioned into N^{n_r} cells. A single value is selected randomly from each interval, producing N sample values for each input variable. The values are randomly matched to create N sets from the N^{n_r} space with respect to the density of each interval for the N simulation runs. The advantage of the LHS approach is that the random samples are generated from all the ranges of possible values.

3. Multi-objective optimization

In many practical applications a single criterion rarely gives a representative measure of the actual structural performance, as several conflicting and usually incommensurable criteria have to be taken into account simultaneously. The optimization problem with more than one objective is called as multi-criteria, multi-objective or vector optimization problem [4].

3.1. Conflict and criteria

The engineer looking for the optimum design of a structure is faced with the question of selecting the most suitable criteria for measuring the economy, strength, serviceability or any other factor that affects

the performance of the structure. Any quantity that has an influence on the structural performance can be considered as a criterion. One important basic property in the multi-criterion formulation is the conflict that should exist among the various criteria. Only those quantities that are conflicting with each other should be treated as independent criteria whereas the others can be combined into a single criterion representing the whole group.

Two functions f_i and f_j are called *locally collinear* with no conflict at point \mathbf{s} if there is $c > 0$ such that $\nabla f_i(\mathbf{s}) = c \nabla f_j(\mathbf{s})$. Otherwise, the functions are called *locally conflicting* at point \mathbf{s} . According to this definition any two criteria are locally conflicting at a point of the design space if their maximum improvement is achieved in different directions. On the other hand, the two functions f_i and f_j are called *globally conflicting* in the feasible region \mathcal{F} of the design space if the two optimization problems $\min\{f_i(\mathbf{s}) : \mathbf{s} \in \mathcal{F}\}$ and $\min\{f_j(\mathbf{s}) : \mathbf{s} \in \mathcal{F}\}$ have different optimal solutions.

3.2. Formulation of the multi-objective optimization problem

In general, the mathematical formulation of a multi-objective problem that includes a set of n design variables, a set of m objective functions and a set of k constraint functions can be defined as follows

$$\begin{aligned} \min_{\mathbf{s} \in \mathcal{F}} \quad & [f_1(\mathbf{s}), f_2(\mathbf{s}), \dots, f_m(\mathbf{s})]^T \\ \text{subject to} \quad & g_j(\mathbf{s}) \leq 0 \quad j = 1, \dots, k, \\ & \mathbf{s}_i \in R^d, \quad i = 1, \dots, n, \end{aligned} \quad (7)$$

where the vector $\mathbf{s} = [s_1 \ s_2 \ \dots \ s_n]^T$ represents a design variable vector and \mathcal{F} is the feasible region, a subspace of the design space R^n for which the constraint functions $g(\mathbf{s})$ are satisfied

$$\mathcal{F} = \{\mathbf{s} \in R^n | g_j(\mathbf{s}) \leq 0 \quad j = 1, \dots, k\} \quad (8)$$

If the m objective functions are globally conflicting, there is no unique point that would represent the optimum for all m objectives. Thus, the common optimality condition used in single-objective optimization must be replaced by a new concept, the so called *Pareto optimum*: a design vector $\mathbf{s}^* \in \mathcal{F}$ is a Pareto optimum for the problem of Eq. (7) if and only if there is no other design vector $\mathbf{s} \in \mathcal{F}$ such that

$$\begin{aligned} f_i(\mathbf{s}) &\leq f_i(\mathbf{s}^*) \quad \text{for } i = 1, \dots, m, \\ \text{with } f_j(\mathbf{s}) &< f_j(\mathbf{s}^*) \quad \text{for at least one objective } j. \end{aligned} \quad (9)$$

The geometric locus of the Pareto optimum solutions is called Pareto front curve and represents the solution of the optimization problem with multiple objectives. In practical applications however, the designer seeks for a unique final solution to be implemented in practice, thus a compromise should be made among the available Pareto optimal solutions.

3.3. Domination and non-domination

In single objective optimization problems the feasible set \mathcal{F} can be ordered univocally according to the value of the objective function. For example, in the case of the minimization problem of $f(\mathbf{s})$, two solutions \mathbf{s}_a and $\mathbf{s}_b \in \mathcal{F}$ can be classified using the condition $f(\mathbf{s}_a) < f(\mathbf{s}_b)$. In a multi-objective optimization problem two solutions \mathbf{s}_a and $\mathbf{s}_b \in \mathcal{F}$ cannot be classified in a univocal manner. The concept of the Pareto dominance is used for assessing the two solutions, which for a minimization problem can be defined as follows

$$\begin{aligned} \mathbf{s}_a \text{ dominates } \mathbf{s}_b & \text{ if } f_i(\mathbf{s}_a) < f_i(\mathbf{s}_b) \quad \forall i = 1, \dots, m, \\ \mathbf{s}_a \text{ weakly dominates } \mathbf{s}_b & \text{ if } f_i(\mathbf{s}_a) \leq f_i(\mathbf{s}_b) \quad \forall i = 1, \dots, m, \\ \mathbf{s}_a \text{ is indifferent to } \mathbf{s}_b & \text{ otherwise.} \end{aligned} \quad (10)$$

Using the definition of Eq. (10), the Pareto optimality can be stated as follows: A solution $\mathbf{s}^* \in \mathcal{F}$ is Pareto optimal if it is not dominated by any other feasible design.

3.4. Solving the multi-objective optimization problem

Several methods have been proposed for treating structural multi-objective optimization problems [3,10,13]. According to Marler and Arora [14] these methods can be divided into: (i) methods with a priori articulation of preferences, (ii) methods with a posteriori articulation of preferences and (iii) methods with no articulation of preferences. The proposed Cascade Evolutionary Algorithm-based (CEA) multi-objective optimization scheme belongs to the first category. This algorithm is compared to the Linear Weighting Sum method (LWS), also belonging to the a priori articulation of preferences. The LWS method, due to its simplicity, is the most widely implemented method for solving such problems. In both methods employed, the problem in finding the Pareto front curve is reduced into a sequence of parameterized single-objective optimization *subproblems*, using scalarizing functions.

In general, when using scalarizing functions, locally Pareto optimal solutions are obtained. Global Pareto optimality can be guaranteed only when the objective functions and the feasible region are both convex or quasi-convex and convex, respectively. For non-convex cases, such as the majority of structural multi-objective optimization problems, a global single objective optimizer must be implemented. Evolutionary Algorithms (EA) are considered as global optimizers since they are not prone to being trapped in local optima and therefore can be considered as the most reliable methods in approaching the global optimum for non-convex constrained optimization problems. For this reason an evolutionary algorithm has been considered in this study for the solution of the sequence of the parameterized single objective optimization problems.

The quality of the Pareto front curve obtained can be assessed according to the following rules:

- Distance from the exact Global Pareto front curve.
- Number of Pareto optimum solutions.
- Distribution of the Pareto optimum solutions along the front curve.

3.4.1. Linear Weighting Sum method

In the LWS method all the objectives are combined into a scalar parameterized function by using weighting coefficients. If w_i , $i = 1, 2, \dots, m$ are the weighting coefficients, the problem of Eq. (7) can be written as follows:

$$\min_{\mathbf{s} \in \mathcal{F}} \sum_{i=1}^m w_i \frac{|f_i(\mathbf{s}) - z_i^*|}{f_i(\mathbf{s})}, \quad (11)$$

where z_i^* is the utopian objective function value. With no loss of generality the following normalization of the weighting coefficients is employed:

$$\sum_{i=1}^m w_i = 1. \quad (12)$$

The values of the weighting coefficients can be adjusted according to the importance of each criterion. Every combination of the weighting coefficients correspond to a single Pareto optimal solution, thus by performing a sequence of optimization runs using different weighting coefficients a set of Pareto optimal solutions is obtained.

3.4.2. Non-dominant multi-objective search using the Tchebycheff metric

The proposed Cascade Evolutionary Algorithm (CEA)-based optimization scheme combines the CEA methodology with a non-dominance search and the Tchebycheff metric.

3.4.2.1. Augmented weighted Tchebycheff problem. The augmented weighted Tchebycheff method belongs to the methods with a priori articulation of the preferences for treating the multi-objective optimization problem and, unlike the linear weighting sum method, can be applied effectively to convex as well as to non-convex problems [17]. The weighted Tchebycheff metric can generate any optimal solution, to any type of optimization problem [23]. In order to overcome weakly Pareto optimal solutions, the Tchebycheff method formulates the distance minimization problem as a weighted Tchebycheff problem

$$\min_{\mathbf{s} \in \mathcal{F}} \max_{i=1, \dots, m} \left[w_i \frac{|f_i(\mathbf{s}) - z_i^*|}{f_i(\mathbf{s})} + \rho \sum_{i=1}^m \frac{|f_i(\mathbf{s}) - z_i^*|}{f_i(\mathbf{s})} \right], \quad (13)$$

where ρ is a sufficiently small positive scalar (in this work $\rho = 0.1$). The weight parameters w_i are random numbers, uniformly distributed between 0 and 1. These weight parameters have to fulfil the requirement of Eq. (12), if not, they are updated according to the following expression:

$$w_i = \begin{cases} w_i + \frac{1 - \sum_i^m w_i}{\sum_i^m w_i} w_i, & \text{if } \sum_i^m w_i \neq 1, \\ w_i, & \text{if } \sum_i^m w_i = 1. \end{cases} \quad (14)$$

3.4.2.2. CEA-based multi-objective optimization scheme. It is generally accepted that there is still no unique optimization algorithm capable of handling with equal efficiency all existing optimization problems. Cascade optimization attempts to alleviate this deficiency by applying a multi-stage procedure in which various optimizers are implemented successively. In the present work the idea of cascading is implemented in the EA-context (CEA) for solving multi-objective structural optimization problems. In particular, the CEA method is employed for the solution of the sequence of parameterized single objective optimization problems. The resulting cascade evolutionary procedure consists of a number of optimization stages (*csteps*), each of which employs the same EA optimizer. In order to differentiate the search paths followed by the same optimization algorithm during the cascade stages, the initial conditions of the individual optimization runs are suitably controlled by using at each stage a different initial design (each stage initiates from the solution of the previous stage) and a different seed for the random number generator of the EA procedure [1].

A non-dominant search is performed in the context of the CEA and the Tchebycheff metric in the sense that all non-dominated solutions attained so far are kept in a set called temporary Pareto set. It was mentioned before that the multi-objective optimization problems are decomposed into *subproblems* which are solved with independent runs (*nruns* in total) of the CEA methodology. Each subproblem is independent from the other and therefore all subproblems can be dealt with simultaneously. Furthermore, in every global generation a non-dominant search is applied for updating the temporary Pareto set. The global generation is achieved when all local generations of the independent CEA runs are completed. According to this procedure in every global generation a local Pareto front is produced which approaches the global one.

The optimization algorithm proposed in this study is denoted as: non-dominant CEATm($\mu + \lambda$)_{nruns, csteps} where μ , λ are the number of the parent and offspring vectors used in the ES optimization strategy, *nruns* is the number of independent CEA runs and *csteps* is the number of cascade stages employed. The proposed optimization scheme can easily be applied in two parallel computing levels, an external and an internal one. As it was mentioned earlier the multi-objective optimization problem is converted into a series of single objective optimization problems. The solution of each subproblems can be performed concurrently

constituting the *external parallel computing level*. On the other hand, the utilization of the natural parallelization capabilities of the CEA methodology within each independent run defines the *internal parallel computing level*. The basic steps inside an independent run of the multi-objective algorithm, as adopted in this study, are the following:

Independent run $i, i = 1, \dots, \text{nrun}$

Generate the weight coefficients $w_{i,j}, j = 1, \dots, m$ of the Tchebycheff metric. Check if the requirement of Eq. (12) is fulfilled, if not change the weight parameters using Eq. (14).

CEATm loop

1. *Initial generation:*

1a. *Generate \mathbf{s}_k ($k = 1, \dots, \mu$) vectors*

1b. *Structural analysis step*

1c. *Evaluation of the Tchebycheff metric, Eq. (13)*

1d. *Constraint check: if satisfied $k = k + 1$ else $k = k$. Go to step 1a*

2. *Global non-dominant search:* Check if global generation is accomplished. If yes, then non-dominant search is performed according to Eq. (10), else wait until global generation is accomplished

3. *New generation:*

3a. *Generate \mathbf{s}_ℓ ($\ell = 1, \dots, \lambda$) vectors*

3b. *Structural analysis step*

3c. *Evaluation of the Tchebycheff metric, Eq. (13)*

3d. *Constraint check: if satisfied $\ell = \ell + 1$ else $\ell = \ell$. Go to step 3a*

4. *Selection step:* selection of the next generation parents according to $(\mu + \lambda)$ or (μ, λ) scheme

5. *Global non-dominant search:* Check If global generation is accomplished. If yes, then non-dominant search is performed according to Eq. (10), else wait until global generation is accomplished

6. *Convergence check:* If satisfied stop, else go to step 5

End of CEATm loop

End of Independent run i

4. Robust design optimization

In the present study the robust design versus the deterministic-based design optimization of large-scale 3D truss structures is investigated. The random variables chosen are the cross-sectional dimensions of structural members, the material properties of modulus of elasticity E , the yield stress σ_y as well as the applied loading.

4.1. Deterministic-based optimization

In a Deterministic-Based Optimization (DBO) problem the aim is to optimize the performance of the structural system which usually tends to be the minimization of the weight under certain deterministic behavioral constraints. A discrete DBO problem can be formulated in the following form:

$$\begin{aligned} \min \quad & f(\mathbf{s}) \\ \text{subject to} \quad & g_j(\mathbf{s}) \leq 0 \quad j = 1, \dots, k, \\ & \mathbf{s}_i \in R^d, \quad i = 1, \dots, n, \end{aligned} \quad (15)$$

where $f(\mathbf{s})$ is the objective function and $g_j(\mathbf{s})$ are the deterministic constraints. Most frequently these constraints refer to member stresses and nodal displacements or inter-storey drifts for building structures.

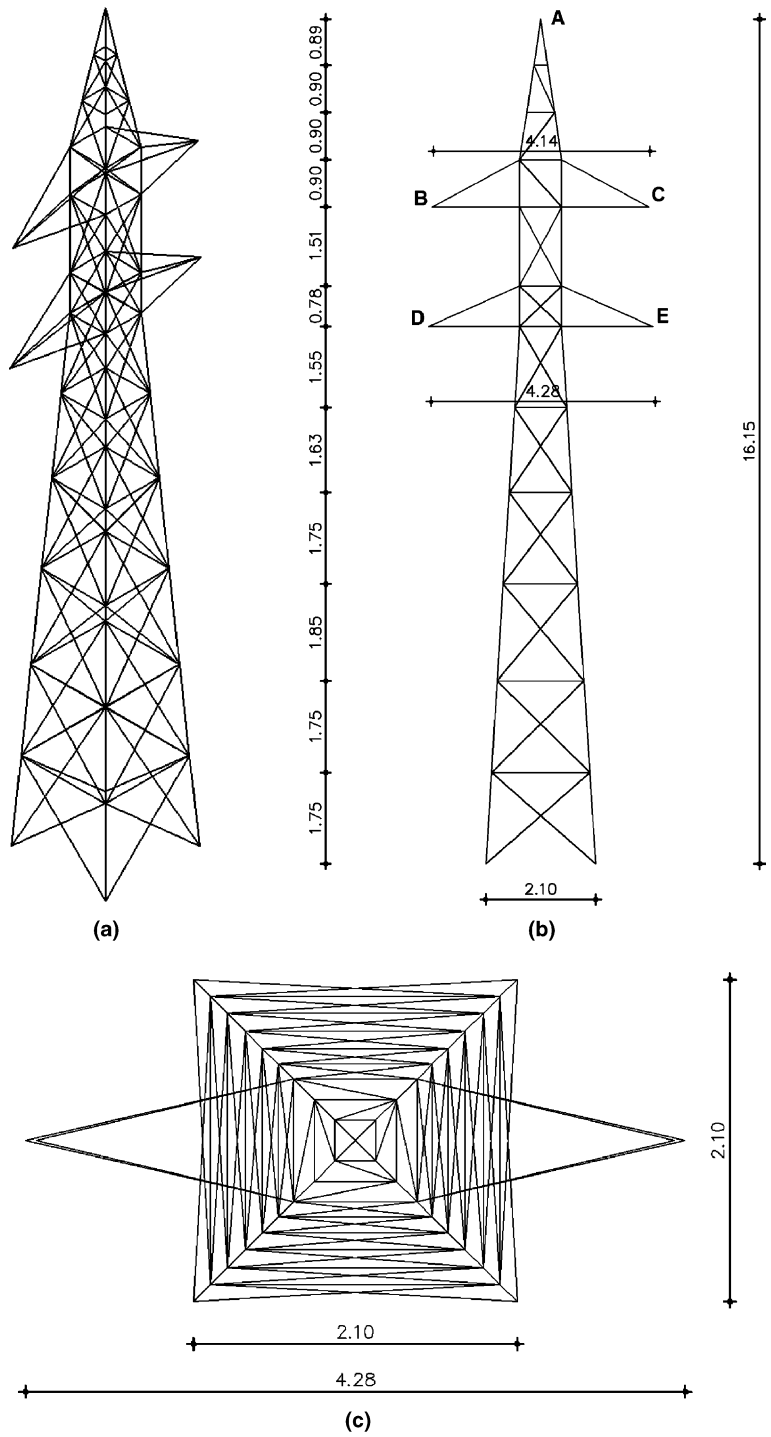


Fig. 1. Transmission tower: (a) 3D view, (b) side view, (c) top view.

In this study three types of constraints are imposed to the sizing optimization problem considered: (i) stress, (ii) compression force (for buckling) and (iii) displacement constraints. The stress constraint can be written as follows

$$\begin{aligned} \sigma_{\max} &\leq \sigma_a, \\ \sigma_a &= \frac{\sigma_y}{1.10}, \end{aligned} \tag{16}$$

where σ_y is the yield stress, σ_{\max} is the maximum axial stress in each element group for all loading cases and σ_a is the allowable axial stress, all taken according to the Eurocode 3 [8] for design of steel structures. For members under compression an additional constraint is used

$$\begin{aligned} |P_{c,\max}| &\leq P_{cc}, \\ P_{cc} &= \frac{P_e}{1.05}, \\ P_e &= \frac{\pi^2 EI}{L_{\text{eff}}^2}, \end{aligned} \tag{17}$$

where $P_{c,\max}$ is the maximum axial compression force for all loading cases, P_e is the critical Euler buckling force in compression, taken as the first buckling mode of a pin-connected member, and L_{eff} is the effective length. The effective length is taken equal to the actual length. Similarly, the displacement constraints can be written as

$$|d| \leq d_a, \tag{18}$$

where d_a is the limit value of the displacement at a certain node or at the maximum nodal displacement.

4.2. Formulation of the robust design optimization problem

In a robust design sizing optimization problem an additional objective function is considered which is related to the influence of the random nature of some structural parameters on the response of the structure. In the present study the aim is to minimize both the weight and the variance of the response of the structure due to the uncertainty of the random parameters. This problem is treated as a two-objective optimization problem using the weighted Tchebycheff metric. The mathematical formulation of the RDO problem implemented in this study is as follows:

$$\begin{aligned} \min \quad & \Phi(\mathbf{s}) \\ \text{subject to} \quad & g_j(\mathbf{s}) \leq 0 \quad j = 1, \dots, k, \\ & \mathbf{s}_i \in R^d, \quad i = 1, \dots, n, \end{aligned} \tag{19}$$

Table 1
Transmission tower: characteristics of the random variables

		Probability density function	Mean value, μ	Standard deviation, σ	σ/μ (%)	95% of values within
E (kN/m ²)	Young's modulus	Normal	2.10E+08	1.50E+07	7.14	(1.81E+08, 2.39E+08)
σ_y (kN/m ²)	Allowable stress	Normal	355000	35500	10.00	(2.85E+05, 4.25E+05)
F (kN)	Nodal loading	Normal	μ_F	$0.05\mu_F$	5	($0.902\mu_F$, $1.098\mu_F$)
L	Legs length	Normal	L_i^a	$0.02L_i$	2	($0.961L_i$, $1.039L_i$)
t	Legs width	Normal	t_i^a	$0.02t_i$	2	($0.961t_i$, $1.039t_i$)

^a Taken from the Equal Angle Section (EAS) table of the Eurocode for every design.

where $\Phi(\mathbf{s})$ is the multi-objective function, which is expressed as

$$\Phi(\mathbf{s}) = \max \left[w_1 \frac{|f(\mathbf{s}) - z_1^*|}{f(\mathbf{s})} + \rho \sum_{i=1}^m \frac{|f(\mathbf{s}) - z_1^*|}{f(\mathbf{s})}, \quad w_2 \frac{|\sigma_{u_i}(\mathbf{s}) - z_2^*|}{\sigma_{u_i}(\mathbf{s})} + \rho \sum_{i=1}^m \frac{|\sigma_{u_i}(\mathbf{s}) - z_2^*|}{\sigma_{u_i}(\mathbf{s})} \right], \quad (20)$$

where $f(\mathbf{s})$ is the weight of the structure and $\sigma_{u_i}(\mathbf{s})$ is the standard deviation of the response of the structure.

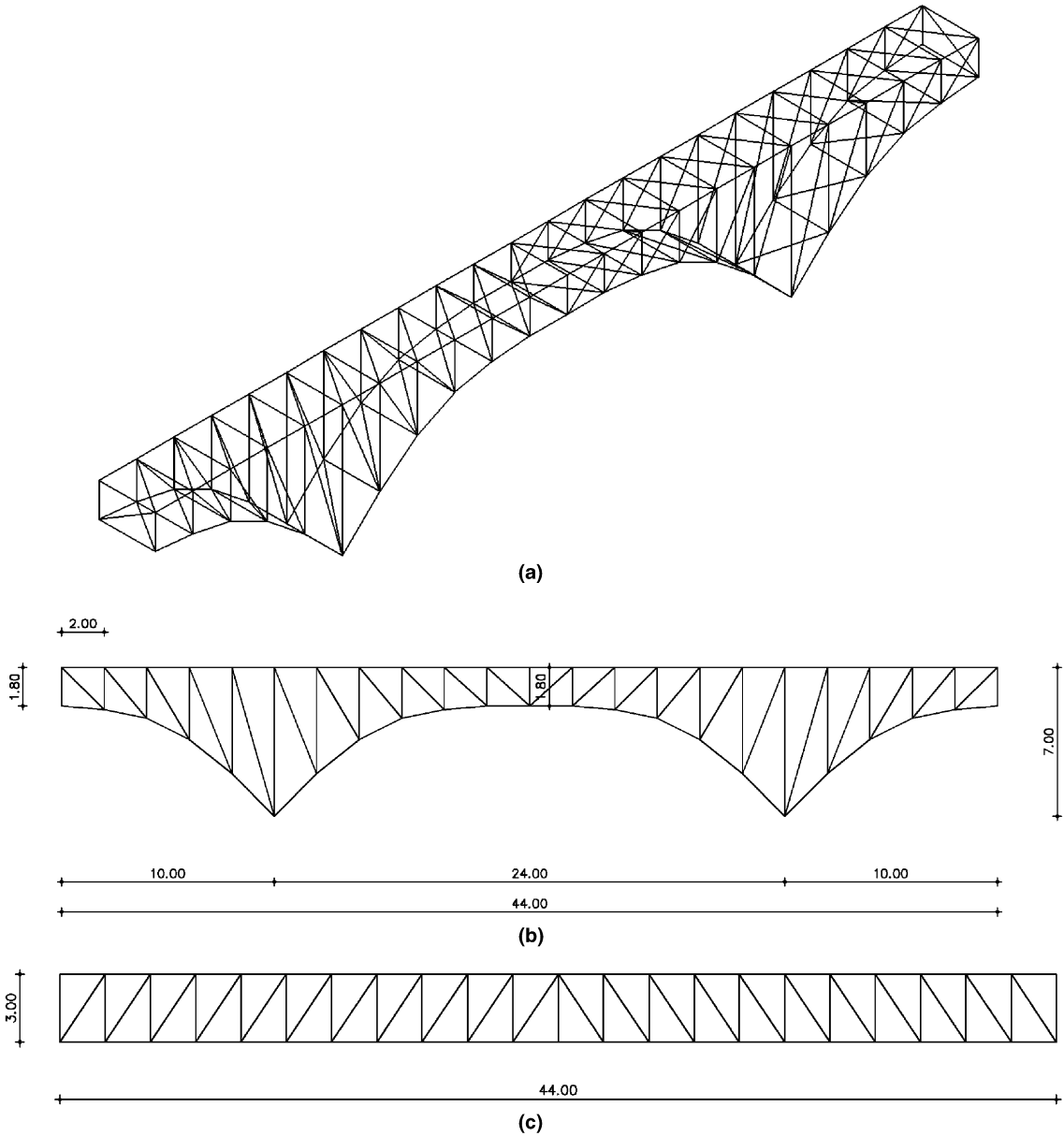


Fig. 2. Truss bridge: (a) 3D view, (b) side view, (c) top view.

5. Numerical tests

The numerical tests examined are performed in three stages. In the first stage the statistical methods used for the stochastic analysis are verified. The number of LHS simulations required for the calculation of the mean value and the standard deviation of the characteristic displacement representing the structural response is compared with the corresponding number required by the basic MCS. In the second stage the advantages of the proposed non-dominant CEATm method over the LWS method are demonstrated through the comparison of the Pareto front curves obtained. While in the third stage, the differences between DBO and RDO optimum designs, in terms of the final structural weight, the variance of response, the probability of violation of the constraints and the probability of failure, are illustrated in two 3D truss structures.

The first test example is the transmission tower, depicted in Fig. 1, together with its geometric characteristics. The design variables considered are the dimensions of the structural members, divided into seven groups, taken from the Equal Angle Section (EAS) table of the Eurocode. For each design variable, two stochastic variables are assigned: The length L and the width t of the legs of the section. The following loading vectors $[F_x, F_y, F_z]$ in kN are applied to the structure: node A $[-8.51, 0.00, -4.82]$, node B $[-9.77, 0.00, -5.36]$, node C $[-9.77, 0.00, -5.36]$, node D $[-10.70, 0.00, -5.36]$ and node E $[-10.70, 0.00, -5.36]$, while the type of probability density function, the mean value, and the variance of the random parameters are given in Table 1. A constraint maximum deflection of 200 mm is imposed.

The second test example is the pedestrian truss bridge shown in Fig. 2. The design variables considered are the dimensions of the structural members divided into 12 groups, taken from the double Equal Angle Section (double EAS) table of the Eurocode. For each design variable, three stochastic variables are assigned: the length L , the width t of the legs and the distance d between the two identical equal angle sections. The applied loading consists of: (i) distributed load equal to 5 kN/m² (dead load), (ii) live loads (visiting vehicle) and (iii) wind actions according to Eurocode [6,7]. The type of probability density function, the mean value, and the variance of the random parameters are given in Table 2, while a maximum deflection constraint of 200 mm is imposed on the nodes of the structure.

5.1. Efficiency of the stochastic analysis method

In the first stage of the numerical study, the performance of the LHS procedure in calculating the statistical parameters required during the RDO procedure compared to the basic MCS is examined. For both test examples it is examined the influence of the number of simulations on the computed value of the

Table 2
Truss bridge: characteristics of the random variables

		Probability density function	Mean value, μ	Standard deviation, σ	σ/μ (%)	95% of values within
E (kN/m ²)	Young's modulus	Normal	2.10E+08	1.50E+07	7.14	(1.81E+08, 2.39E+08)
σ_y (kN/m ²)	Allowable stress	Normal	355000	35500	10.00	(2.85E+05, 4.25E+05)
F_P (kN)	Permanent loading	Normal	μ_{F_P}	$0.05\mu_{F_P}$	5	($0.902\mu_{F_P}$, $1.098\mu_{F_P}$)
F_L (kN)	Live loading	Normal	μ_{F_L}	$0.05\mu_{F_L}$	5	($0.902\mu_{F_L}$, $1.098\mu_{F_L}$)
F_W (kN)	Wind loading	Normal	μ_{F_W}	$0.10\mu_{F_W}$	10	($0.804\mu_{F_W}$, $1.196\mu_{F_W}$)
L	Legs length	Normal	L_i^a	$0.02L_i$	2	($0.961L_i$, $1.039L_i$)
t	Legs width	Normal	t_i^a	$0.02t_i$	2	($0.961t_i$, $1.039t_i$)
d	EAS section distance	Normal	d_i^a	$0.02d_i$	2	($0.961d_i$, $1.039d_i$)

^a Taken from the double Equal Angle Section (double EAS) table of the Eurocode for every design.

variance of characteristic displacements: The top horizontal displacement for the Transmission Tower and the vertical deflection of the middle node for the Pedestrian Bridge. The results, for randomly selected designs, shown in Figs. 3 and 4 for the two test examples, respectively, demonstrate the efficiency of the implemented LHS procedure. It can be seen from Fig. 3 that for the transmission tower, 100 LHS compared to

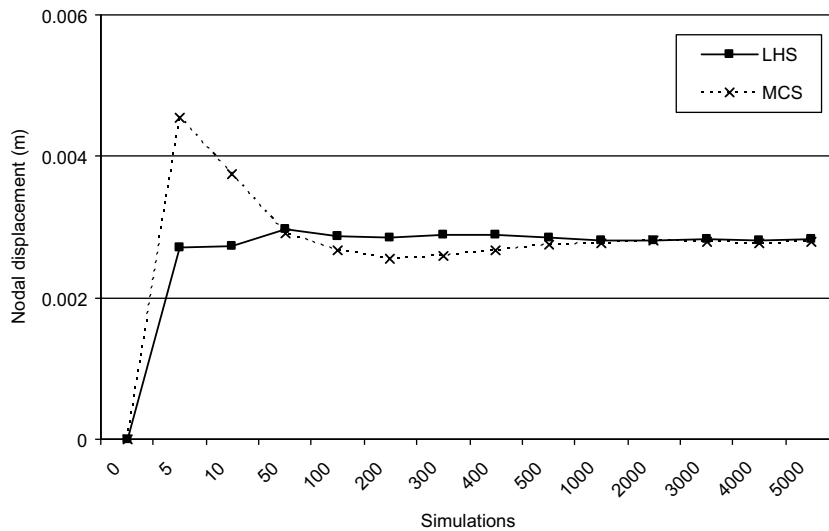


Fig. 3. Transmission tower: efficiency of the LHS compared to the MCS in calculating the standard deviation of the structural response.

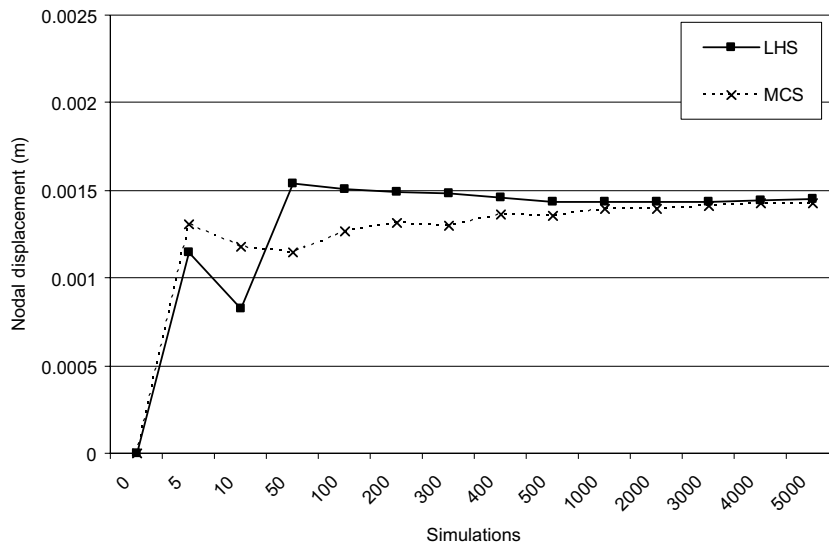


Fig. 4. Truss bridge: efficiency of the LHS compared to the MCS in calculating the standard deviation of the structural response.

500 MCS simulations are required in order to calculate the standard deviation of the structural response, while for the truss bridge 100 LHS compared to 1000 MCS simulations are required. It has to be stated that the number of simulations required may vary depending on the type of the structure, the loading conditions and the statistical characteristics of the structural parameters.

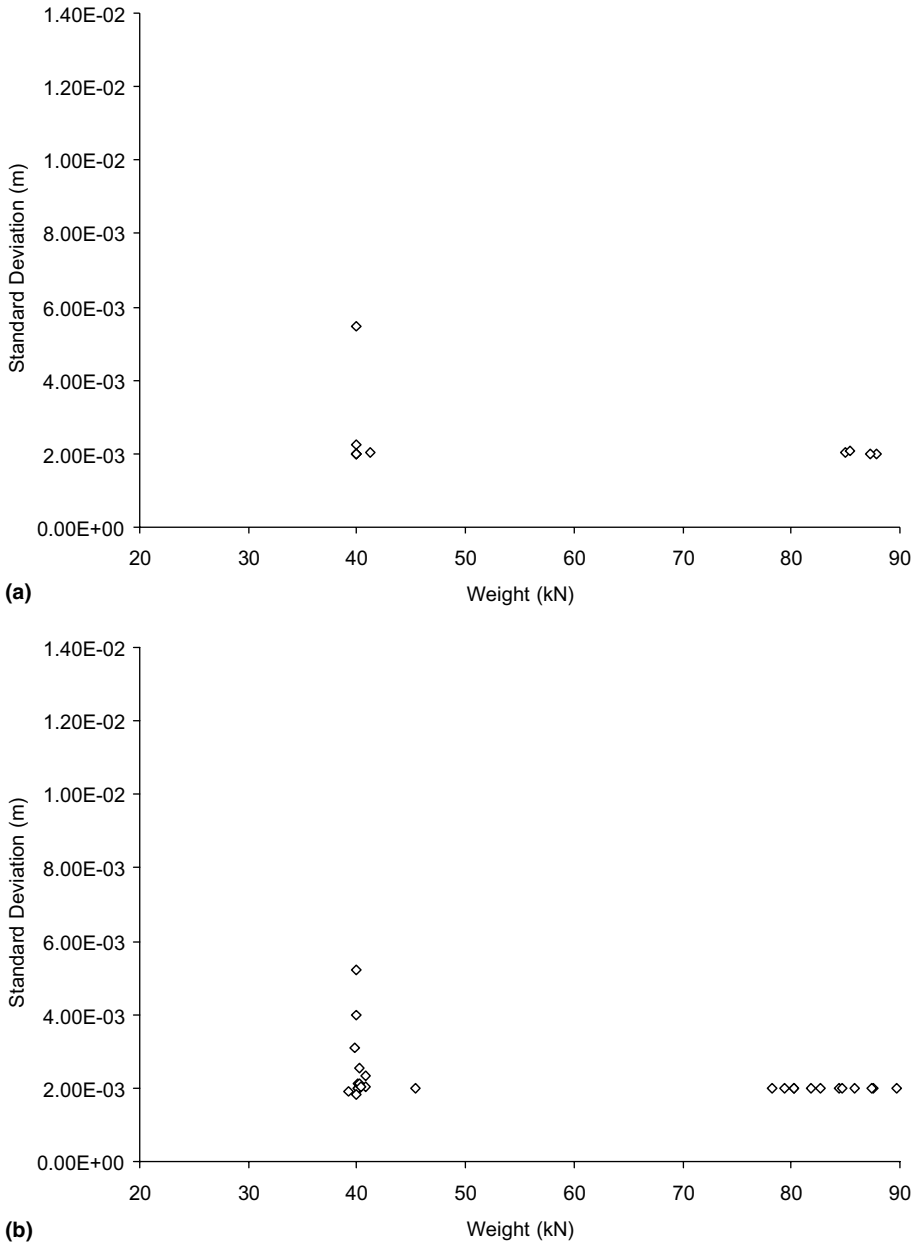


Fig. 5. Transmission tower: the Pareto front curve obtained with LWS (a) 10 points, (b) 30 points.

5.2. Comparison between LWS and CEATm

In the second stage of this study the advantages of the cascade evolutionary multi-objective optimization scheme using the Tchebycheff metric are demonstrated over the linear weighing sum method. As it was mentioned in Section 3.4 the quality of the Pareto front curve can be assessed by the number of Pareto optimum solutions obtained and their distribution along the front curve. Well distributed solutions along the curve is an indication of the efficiency of the multi-objective optimization method employed. The main drawback of the multi-objective optimization methods using scalarizing functions, such as the LWS, is that it is difficult to fulfil these two requirements.

For the comparative study performed in this study the robust design optimization problem considered has been solved with the LWS method and the proposed non-dominant CEATm multi-objective optimization scheme. For both test examples the LWS method has been implemented through two different runs with 10 and 30 points using the $ES(\mu + \lambda)$ optimization algorithm where $\mu = \lambda = 5$ are the number of parents and offsprings, respectively. For the non-dominant CEATm $(\mu + \lambda)_{nrun, csteps}$ optimization scheme the corresponding parameters are $\mu = \lambda = 5$, $nrun = 10$ and $csteps = 3$. The resultant Pareto front curves, for the first test example, are depicted in Figs. 5 and 6 for the LWS and the CEATm, respectively. The horizontal axis corresponds to the structural weight and the vertical axis to the standard deviation of the characteristic node displacement. For the second test example the corresponding front curves are depicted in Figs. 7 and 8.

The RDO multi-objective optimization problem is non-convex and the weakness of the LWS is obvious from the front curves of Figs. 5 and 7. Well distributed pairs of weighting coefficients does not correspond to equally well distributed Pareto optimum solutions along the front curve. On the other hand, the proposed CEATm optimization scheme manages to generate the Pareto front curve having a good distribution of the Pareto solutions along the front curve, as can be seen in Figs. 6 and 8.

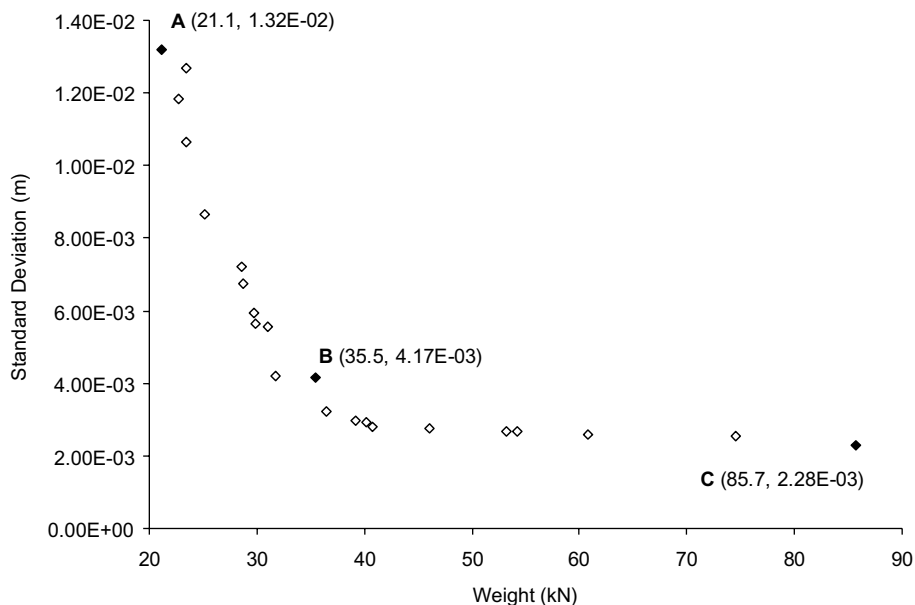


Fig. 6. Transmission tower: the Pareto front curve obtained with the non-dominant CEATm.

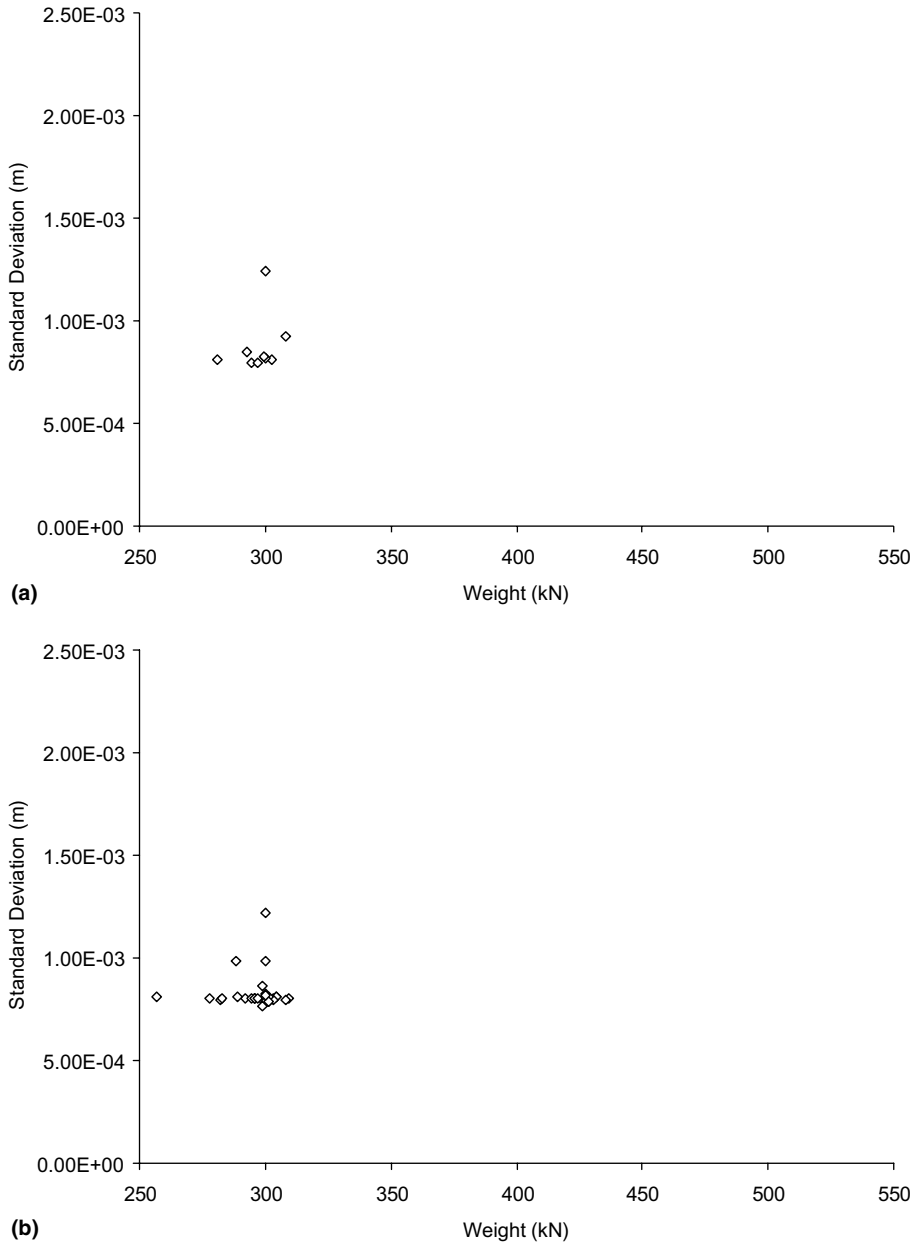


Fig. 7. Truss bridge: the Pareto front curve obtained with LWS (a) 10 points, (b) 30 points.

5.3. Comparison between DBO and RDO solutions

In the third stage of this study the difference between DBO and RDO optimum designs is demonstrated in terms of the structural weight, the variance of the response and the probability of violation of the constraints. The resultant Pareto front curves for the two test examples, when the proposed optimization scheme is used, are shown in Figs. 6 and 8, respectively. The two ends of the Pareto front curve represent

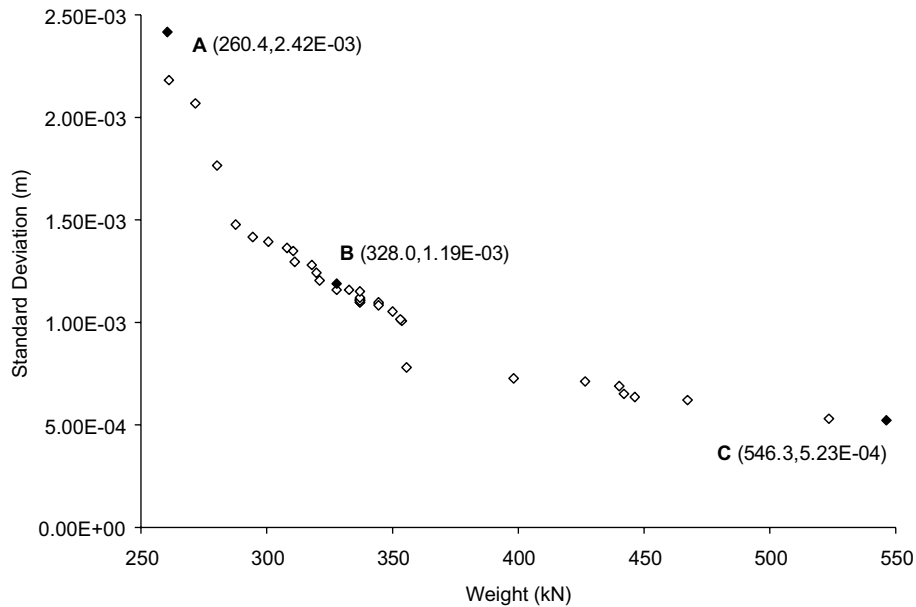


Fig. 8. Truss bridge: the Pareto front curve obtained with the non-dominant CEATm.

two extreme designs. Point A correspond to the deterministic-based optimum where the weight of the structure is the dominant criterion. Point C is the optimum when the standard deviation of the response is considered as the dominant criterion. The intermediate Pareto optimal solutions are compromise solutions between these two extreme optimum designs under conflicting criteria.

In Tables 3 and 4 comparisons are performed for the three optimum designs A, B and C of Figs. 6 and 8. The RDO(B) optimum design is achieved considering a compromise between the weight and the standard deviation. An important outcome of this investigation is that the DBO optimum design violates the constraints with probability equal to 1.1% and 0.85% and probability of failure equal to 0.6% and 0.23%, respectively for the two test examples considered. On the other hand, the probability of violation and the probability of failure, in the case of the compromise optimum design B, are computed one to two orders

Table 3
Transmission tower: characteristic optimal solutions

	DBO (A) ($L \times t$) ^a	RDO (B) ($L \times t$) ^a	RDO (C) ($L \times t$) ^a
Sec ₁	80 × 8	110 × 10	150 × 12
Sec ₂	70 × 7	150 × 14	160 × 15
Sec ₃	80 × 6	100 × 8	180 × 16
Sec ₄	70 × 9	80 × 6	150 × 12
Sec ₅	70 × 6	80 × 8	150 × 12
Sec ₆	75 × 7	90 × 7	150 × 12
Sec ₇	75 × 8	100 × 8	160 × 17
Weight (kN)	21.1	35.5	85.7
Standard deviation (m)	1.32×10^{-02}	4.17×10^{-03}	2.28×10^{-03}
p_{viol} (%)	1.1×10^0	7.0×10^{-2}	2.0×10^{-3}
p_f (%)	0.6×10^0	1.0×10^{-2}	0.8×10^{-3}

^a Taken from the Equal Angle Section (EAS) table of the Eurocode for every design.

Table 4
Truss bridge: characteristic optimal solutions

	DBO (A) ($L \times t - d$) ^a	RDO (B) ($L \times t - d$) ^a	RDO (C) ($L \times t - d$) ^a
Sec ₁	100 × 10–20	150 × 15–20	150 × 15–20
Sec ₂	100 × 10–20	150 × 15–18	200 × 20–20
Sec ₃	120 × 12–18	120 × 12–18	180 × 15–20
Sec ₄	100 × 10–20	120 × 12–20	150 × 15–20
Sec ₅	120 × 12–20	100 × 10–20	120 × 12–20
Sec ₆	100 × 10–20	100 × 10–20	120 × 12–20
Sec ₇	120 × 12–20	120 × 12–18	180 × 15–20
Sec ₈	100 × 10–20	100 × 10–20	200 × 20–20
Sec ₉	100 × 10–20	100 × 10–20	150 × 15–20
Sec ₁₀	100 × 10–20	100 × 10–20	200 × 20–20
Sec ₁₁	100 × 10–20	100 × 10–20	120 × 12–20
Sec ₁₂	100 × 10–18	100 × 10–20	100 × 10–20
Weight (kN)	260.4	328.0	546.3
Standard deviation (m)	2.42×10^{-03}	1.19×10^{-03}	5.23×10^{-04}
p_{viol} (%)	8.5×10^{-1}	1.3×10^{-2}	1.0×10^{-3}
p_f (%)	2.3×10^{-1}	0.7×10^{-2}	1.4×10^{-4}

^a Taken from the double Equal Angle Section (double EAS) table of the Eurocode for every design.

of magnitude lower compared to those corresponding to DBO designs. As a consequence of this reduced probability of violation and failure, an increase of 70% and 30% on the optimum weights achieved is observed in the case of RDO compared to the DBO. The value of the probability of violation is significantly lower in the case of optimum design C where the corresponding probabilities are 0.002% and 0.001% for the two test examples, respectively. However, the optimum weights achieved are four and two times more than the one obtained with the DBO formulation.

The hardware platform that was used in this work for the parallel computing implementation consists of a PC cluster with 25 nodes Pentium III in 500 Mhz interconnected through Fast Ethernet, with every node in a separate 100Mbit/s switch port. Message passing is performed with the programming platforms PVM working over FastEthernet. Two parallel processing schemes have been considered: *Parallel 1* corresponding to the exploitation of the parallel implementation of the optimization scheme and *Parallel 2* corresponding to the parallel implementation of the stochastic analysis involved in the optimization procedure. The computational performance for obtaining the multi-objective RDO Pareto front curve is compared in Tables 5 and 6, for the two test examples. The solution of the single-objective DBO(A) and RDO(C) problems, in sequential and parallel computing environments is examined. It can be seen that the computational time required for obtaining the RDO(C) optimum solutions is two orders of magnitude more than the corresponding time required to obtain the DBO(A) optimum solutions in sequential computing environment. This difference is reduced to one order of magnitude in parallel computing environment.

Table 5
Transmission tower: computational performance

Formulation	Optimization scheme	Generations	FE analyses	Time (s)		
				Sequential	Parallel 1 ^a	Parallel 2 ^a
DBO (A)	CEA(5 + 5)	103	627	63	19	–
RDO (C)	CEATm(5 + 5) _{1,3}	109	576	5214	349	229
RDO Pareto front curve	CEATm(5 + 5) _{10,3}	947	5528	51092	3127	2259

^a In 25 processors.

Table 6
Truss bridge: computational performance

Formulation	Optimization scheme	Generations	FE analyses	Time (s)		
				Sequential	Parallel 1 ^a	Parallel 2 ^a
DBO (A)	CEA(5 + 5)	114	500	91	31	–
RDO (C)	CEATm(5 + 5) _{1,3}	103	529	8643	552	368
RDO Pareto front curve	CEATm(5 + 5) _{10,3}	863	4372	70673	4209	3055

^a In 25 processors.

6. Conclusions

With the proposed multi-objective optimization scheme a uniform distribution of the Pareto optimum solutions along the front curve is achieved which is an indication of the efficiency of the optimization procedure. For the robust design optimization problems considered the proposed non-dominant CEATm multi-objective optimization methodology manages to generate the Pareto front curve with a good distribution of the Pareto solutions along the front curve.

The results obtained with the deterministic and the robust design optimization formulation underline the importance of minimizing the variance of the structural response when uncertain parameters are taken into account. For the test examples considered in this study, the probability of constraint violation of the DBO designs is computed two orders of magnitude greater than the corresponding probabilities for the RDO designs when the standard deviation of the response is considered as the dominant criterion to be minimized. On the other hand, the computational cost required for obtaining the RDO designs is two orders of magnitude in sequential and one order of magnitude in parallel computing environment less than the corresponding computing cost required for obtaining the RDO optimum solutions.

In the computational framework of robust design optimization of real-scale structures it is also shown the efficiency of the Latin hypercube sampling, requiring about a hundred of samples, in calculating the necessary statistical parameters. This part of the optimization procedure is very crucial since the computational cost of the RDO procedure is dependent directly on the number of simulations, while the reliability of results obtained from the RDO procedure is influenced by the accuracy of the calculation of the statistical parameters.

References

- [1] D.C. Charnpis, N.D. Lagaros, M. Papadrakakis, Multi-database exploration of large design spaces in the framework of cascade evolutionary structural sizing optimization, *Comput. Methods Appl. Mech. Engrg.* 194 (30–33) (2005) 3315–3330.
- [2] W. Chen, K. Lewis, A robust design approach for achieving flexibility in multidisciplinary design, *AIAA Journal* 37 (8) (1999) 982–990.
- [3] R.F. Coelho, H. Bersini, Ph. Bouillard, Parametrical mechanical design with constraints and preferences: application to a purge valve, *Comput. Methods Appl. Mech. Engrg.* 192 (39–40) (2003) 4355–4378.
- [4] C.A. Coello Coello, An updated survey of GA-based multi-objective optimization techniques, *ACM Computing Surveys* 32 (2) (2000) 109–143.
- [5] I. Doltsinis, Z. Kang, Robust design of structures using optimization methods, *Comput. Methods Appl. Mech. Engrg.* 193 (2004) 2221–2237.
- [6] Eurocode 1, Basis of design and actions on structures—Part 2–4: Actions on Structures - Wind actions, CEN, ENV 1991-2-4, 1995.
- [7] Eurocode 1, Basis of design and actions on structures—Part 3: Traffic loads on bridges, CEN, ENV 1991-3, 1995.
- [8] Eurocode 3, Design of steel structures, Part 1.1: General rules for buildings, CEN, ENV 1993-1-1, 1993.
- [9] D.M. Frangopol, C.G. Soares (Eds.), Reliability-oriented optimal structural design, *Reliability Engineering & System Safety* (special issue) 73 (3) (2001) 195–306.

- [10] D. Greiner, J.M. Emperador, G. Winter, Single and multiobjective frame optimization by evolutionary algorithms and the auto-adaptive rebirth operator, *Comput. Methods Appl. Mech. Engrg.* 193 (33–35) (2004) 3711–3743.
- [11] D.-H. Jung, B.-C. Lee, Development of a simple and efficient method for robust optimization, *Int. J. Numer. Meth. Engrg.* 53 (2002) 2201–2215.
- [12] K.-H. Lee, G.-J. Park, Robust optimization considering tolerances of design variables, *Comput. Struct.* 79 (2001) 77–86.
- [13] G.-C. Luh, C.-H. Chueh, Multi-modal topological optimization of structure using immune algorithm, *Comput. Methods Appl. Mech. Engrg.* 193 (36–38) (2004) 4035–4055.
- [14] R.T. Marler, J.S. Arora, Survey of multi-objective optimization methods for engineering, *Struct. Multidisc. Optim.* 26 (6) (2004) 369–395.
- [15] M.D. McKay, R.J. Beckman, W.J. Conover, A comparison of three methods for selecting values of input variables in the analysis of output from a computer code, *Technometrics* 21 (2) (1979) 239–245.
- [16] A. Messac, A. Ismail-Yahaya, Multi-objective robust design using physical programming, *Struct. Multidisc. Optim.* 23 (2002) 357–371.
- [17] K. Miettinen, *Non Linear Multi-objective Optimization*, Kluwer Academic Publishers, 2002.
- [18] M. Papadrakakis, N.D. Lagaros, Reliability-based structural optimization using neural networks and Monte Carlo simulation, *Comput. Methods Appl. Mech. Engrg.* 191 (32) (2002) 3491–3507.
- [19] M. Papadrakakis, V. Plevris, N.D. Lagaros, V. Papadopoulos, Robust design optimization of 3D truss structures using evolutionary computation, 6th WCCM in Conjunction with APCOM'04, Beijing, China, September, 5–10, 2004.
- [20] H.J. Pradlwarter, G.I. Schuëller, C.A. Schenk, A computational procedure to estimate the stochastic dynamic response of large non-linear FE-models, *Comput. Methods Appl. Mech. Engrg.* 192 (7–8) (2003) 777–801.
- [21] E. Sandgren, T.M. Cameron, Robust design optimization of structures through consideration of variation, *Comput. Struct.* 80 (2002) 1605–1613.
- [22] G.I. Schuëller (Ed.), *Computational stochastic structural mechanics and analysis as well as structural reliability*, *Comput. Methods Appl. Mech. Engrg.* (2005) (special issue).
- [23] R.E. Steuer, *Multiple Criteria Optimization: Theory Computation and Applications*, John Wiley & Sons, 1986.